inhibitor (Seglen and Gordon, 1982), and then infected with *M. tuberculosis*. The survival of *M. tuberculosis* in Coro1a KD macrophages was partially restored by treatment with 3-MA (Fig. 3A), suggesting that autophagic processes were involved in the inhibition of mycobacterial survival in Coro1a KD macrophages.

To further analyse the inhibitory mechanism of *M. tuberculosis* survival, we infected macrophages co-transfected with siRNAs for Coro1a and autophagy-related genes with *M. tuberculosis*. Atg3, Atg5 and Beclin1 are well-known autophagy-related proteins that drive the autophagy process (Mizushima and Levine, 2010). The targeting efficiencies of Coro1a and autophagy-related genes in Raw264.7 macrophages were confirmed by immunoblot analysis (Fig. 3E). Silencing of these autophagy-related proteins restored this inhibitory effect on *M. tuberculosis* survival in Coro1a KD macrophages (Fig. 3B–D). These results suggest that the induction of autophagy is involved in the promotion of *M. tuberculosis* eradication in Coro1a KD macrophages.

Autophagosome formation around M. tuberculosis*-containing phagosomes in Coro1a KD macrophages*

To confirm autophagosome formation in Coro1a KD macrophages infected with *M. tuberculosis*, we examined the localization of LC3, an autophagosome marker (Kabeya *et al.*, 2000), by fluorescence microscopy. Coro1a KD or control Raw264.7 macrophages were infected with DsRed-expressing *M. tuberculosis* and stained with anti-LC3 antibody. Only a small population of *M. tuberculosis*-containing phagosomes was LC3-positive in the control macrophages at 6 h post infection (p.i.) (Fig. 4A), supporting previous findings (Gutierrez *et al.*, 2004). LC3 recruitment to the mycobacterial phagosomes was further observed in Coro1a KD macrophages (Fig. 4B). Quantitative analysis revealed that the proportion of LC3-positive mycobacterial phagosomes was $> 30\%$ and $< 10\%$ in Coro1a KD and control macrophages respectively (Fig. 4E). Similar experiments employing LC3 fused with enhanced green fluorescence protein (EGFP-LC3) were also conducted. Raw264.7 macrophage stably expressing EGFP-LC3 were infected with DsRed-expressing *M. tuberculosis* for 2, 6 or 24 h. LC3 again localized to a small population of mycobacterial phagosome in control macrophages (Fig. 4C), while the number of LC3-positive mycobacterial phagosomes increased in Coro1a KD macrophages at 6 h p.i. (Fig. 4D). Quantitative analysis revealed that the proportion of LC3-positive mycobacterial phagosomes in Coro1a KD macrophages was greater than 30% and 20% at 6 h and 24 h p.i., respectively, while such an increase was not observed in control macrophages (Fig. 4F).

The ultrastructure of *M. tuberculosis*-containing phagosomes in Coro1a KD macrophages was also observed by thin-section electron microscopy. In control macrophages, bacilli resided in single-membrane phagosomes (Fig. 5A). In contrast, bacilli were surrounded by multiple membrane structures that were characteristic of autophagic vacuoles (Eskelinen, 2005) in Coro1a KD macrophages (Fig. 5B). We also found mycobacterial phagosomes with internal membranes in Coro1a KD macrophages (Fig. 5C) as previously reported (Gutierrez *et al.*, 2004). Quantitative analysis revealed that the proportion of bacilli associated with autophagic membrane structures reached more than 30% in Coro1a KD macrophages while that in control macrophages was less than 10% at 6 h p.i. (Fig. 5D). Collectively, these fluorescence and electron microscopy results suggest that autophagosome formation is induced around *M. tuberculosis*-containing phagosomes in Coro1a KD macrophages.

Validation of LC3 recruitment to M. tuberculosis*-containing phagosomes in Coro1a KD macrophages*

The recruitment of LC3 to *M. tuberculosis*-containing phagosomes was subsequently investigated in Coro1a KD macrophages treated with 3-MA (Fig. 6A) or simultaneously transfected with siRNA duplexes for autophagy-related genes (Fig. 6B). Both treatments abrogated the induction of LC3 recruitment to mycobacterial phagosomes in Coro1a KD macrophages.

Upon autophagy induction, LC3 is processed from a cytosolic form (LC3-I) to a membrane bound form (LC3-II) (Kabeya *et al.*, 2000). We first attempted to confirm the autophagy induction by immunoblot analysis using whole-cell lysates, but no significant increase in LC3 processing was observed in Coro1a KD and control macrophages infected with *M. tuberculosis* (Fig. 7A and D). We also found that no significant changes of LC3 processing in control or Coro1a KD macrophages infected with *M. tuberculosis* at the different infection rates (Fig. S1). The treatment with NH_4Cl or bafilomycin A1 achieved the similar accumulation of LC3-II in both control and Coro1a KD macrophages infected with *M. tuberculosis* (Fig. 7B and E), suggesting the normal autophagic flux in these macrophages. We next examined the recruitment of LC3 using isolated *M. tuberculosis*-containing phagosomes in Coro1a KD macrophages by immunoblot analysis (Fig. 7C). Enrichment of LC3-II was observed in the phagosomal fraction from Coro1a KD macrophages when compared with that from the control macrophages. Densitometric analysis revealed that the amount of LC3-II in the phagosomal fraction from Coro1a KD macrophages increased to approximately 2.7 times that observed for the control macrophages (Fig. 7F). This biochemical analysis

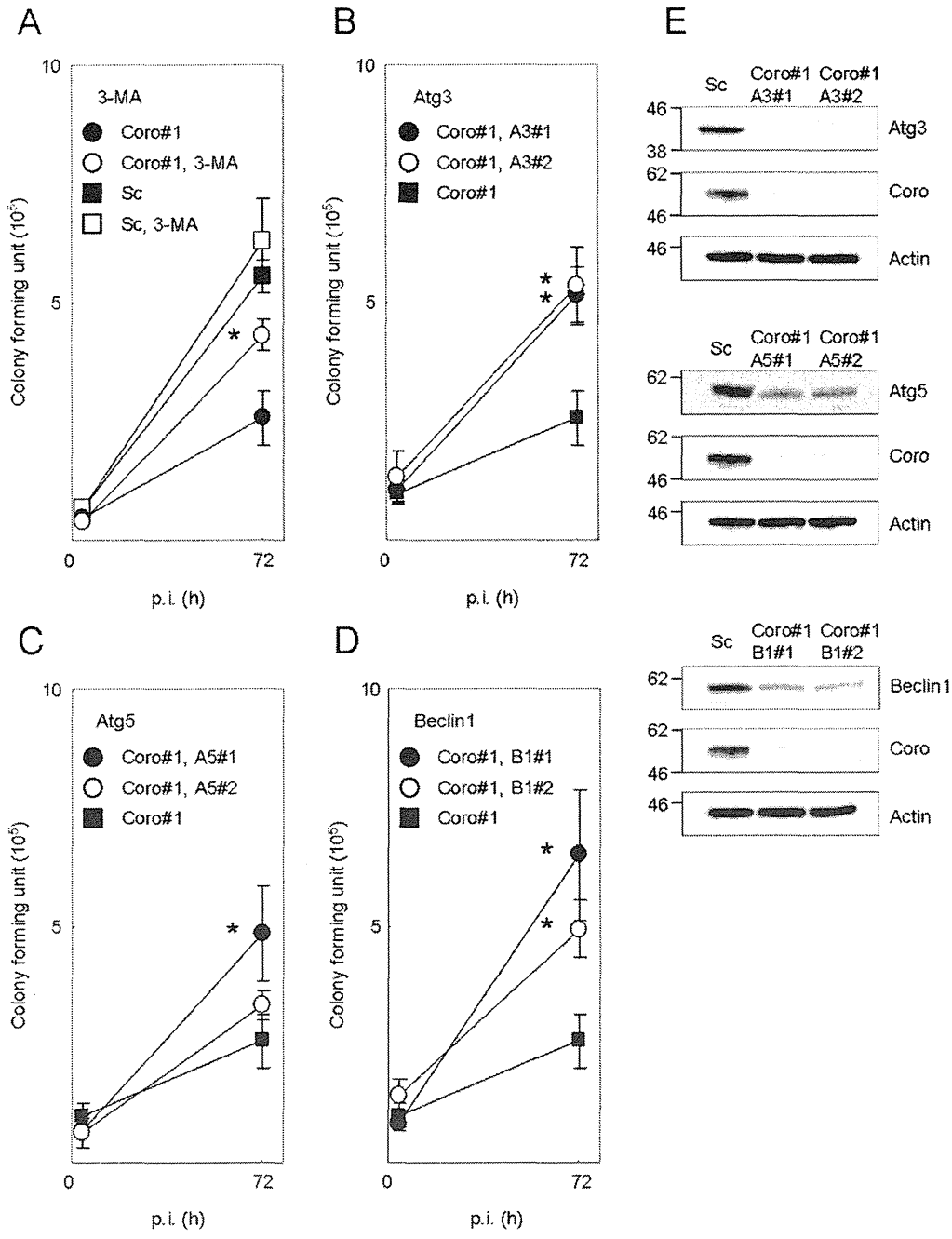

Fig. 3. Treatment with 3-MA or siRNA for autophagy-related genes suppressed the inhibition of *M. tuberculosis* proliferation in Coro1a KD macrophages.

A. Proliferation of *M. tuberculosis* in Coro1a KD macrophages treated with 3-MA. Macrophages transfected with Coro1a-specific or scrambled siRNA were treated with or without 3-MA (10 mM) for 1 h and then infected with *M. tuberculosis*. Viable mycobacteria number was determined by cfu assay at 4 h and 72 h p.i. The data represent the means and SEM of three independent experiments. The numbers of cfu at 72 p.i. in Coro1a KD macrophages treated with or without 3-MA were compared. $*P < 0.05$ (unpaired Student's *t*-test).

B–D. Proliferation of *M. tuberculosis* in macrophages transfected with siRNA for Coro1a and autophagy-related genes. Macrophages were transfected with siRNAs for Coro1a and Atg3 (B), Coro1a and Atg5 (C) or Coro1a and Beclin1 (D). Transfected macrophages were then infected with *M. tuberculosis*. Colony-forming unit assay was performed at 4 h and 72 h p.i. The data represent the means and SEM of three independent experiments. The numbers of cfu at 72 h p.i. in Coro1a KD macrophages transfected with or without siRNA for autophagy-related genes were compared. $*P < 0.05$ (unpaired Student's *t*-test).

E. Immunoblot analysis on the silencing effects of Coro1a and autophagy-related genes. Macrophages were transfected with siRNA for Coro1a and the indicated autophagy-related genes for 48 h. Whole-cell lysates were subjected to SDS-PAGE, followed by immunoblot analysis using the indicated antibodies.

Sc, scrambled; Coro, Coro1a; A3, Atg3; A5, Atg5; B1, Beclin1.

further supports that the recruitment of LC3 to *M. tuberculosis*-containing phagosomes is facilitated by Coro1a depletion in macrophages.

Localization of p62, ubiquitin and LAMP1 to LC3-positive mycobacterial phagosomes in Coro1a KD macrophages

To characterize the LC3-positive mycobacterial phagosomes in Coro1a KD macrophages, we examined the localization of p62/SQSTM1 (p62), ubiquitin and LAMP1 to LC3-positive mycobacterial phagosomes (Fig. 8). Bacteria in cytosols are targeted by the ubiquitin system (Perrin *et al.*, 2004) and the autophagic degradation (Dupont *et al.*, 2009). p62 is involved in targeting intracellular bacteria to the autophagy pathway (Dupont *et al.*, 2009; Zheng *et al.*, 2009) and indispensable for autophagic elimination of mycobacteria in macrophages (Ponpuak *et al.*, 2011). We found that p62 and ubiquitin localized to LC3-positive mycobacterial phagosomes in Coro1a KD macrophages (Fig. 8A and C). The proportion of LC3-positive mycobacterial phagosomes colocalized with p62 and/or ubiquitin increased up to 24 h p.i. (Fig. 8B and D). In addition, the proportion of LC3-positive mycobacterial phagosomes colocalized with LAMP1 also increased up to 24 h p.i. (Fig. 8E and F). These results indicate that p62, ubiquitin and/or LAMP1 are recruited to LC3-positive mycobacterial phagosomes in Coro1a KD macrophages during infection.

Phosphorylation of p38 MAPK is induced by M. tuberculosis *infection in Coro1a KD macrophages*

As mitogen-activated protein kinase (MAPK) signalling pathways are involved in autophagy induction (Esclatine *et al.*, 2009), we next examined which MAPK signalling pathways were affected by *M. tuberculosis* infection in Coro1a KD macrophages (Fig. 9). Macrophages transfected with Coro1a-specific or scrambled siRNA were infected with *M. tuberculosis*, and phosphorylation of ERK1/2, p38 and JNK was investigated by immunoblot analysis. No significant difference in ERK1/2 activation kinetics was detected between control and Coro1a KD macrophages after *M. tuberculosis* infection. JNK activation was not detected in both control and Coro1a KD macrophages (data not shown). In contrast, a significant increase in p38 phosphorylation was observed in Coro1a KD macrophages, while no induction was detected in control macrophages (Fig. 9A).

The recruitment of LC3 to *M. tuberculosis*-containing phagosomes in Coro1a KD macrophages treated with various inhibitors for MAPK signalling pathways was also investigated by imaging analysis. Inhibition of p38 signalling, but not MEK1 or JNK signalling, reduced the proportion of LC3-positive mycobacterial phagosomes in Coro1a KD macrophages (Fig. 9B), further supporting that the p38 MAPK pathway is a target of Coro1a in the inhibition of autophagosome formation around *M. tuberculosis*-containing phagosomes.

Induction of LC3 recruitment to M. tuberculosis*-containing phagosomes in Coro1a KD alveolar macrophages and bone marrow-derived macrophages*

Mycobacterium tuberculosis is inhaled via aerosols into the lung, where alveolar macrophages (AM) are the first line of defence (Russell, 2001; 2007). We investigated whether autophagosome formation around *M. tuberculosis*-containing phagosomes is also induced in AM by Coro1a depletion. MH-S is an AM cell line, in which *M. tuberculosis* can survive and proliferate (Mbawuike and Herscowitz, 1989; Sirakova *et al.*, 2003). MH-S macrophages were transfected with Coro1a siRNA (Fig. 10A) and infected with *M. tuberculosis*. When AM were transfected with scrambled siRNA, LC3 did not localize to mycobacterial phagosomes (data not shown). In contrast, the recruitment of LC3 to mycobacterial phagosomes increased in Coro1a KD AM (Fig. 10B). Quantitative analysis revealed that the proportions of LC3-positive mycobacterial phagosomes were $> 25\%$ and $< 5\%$ in Coro1a KD and control AM respectively (Fig. 10C). We also examined the localization of LC3 to mycobacterial phagosomes in bone marrow-derived macrophages (BMDM) transfected with Coro1a-specific or scrambled siRNA (Fig. 10A). The depletion of Coro1a also induced the recruitment of LC3 to *M. tuberculosis*-containing phagosomes in BMDM (Fig. 10D). Quantitative analysis revealed that approximately 10% and 2% of mycobacterial phagosomes were LC3 positive in Coro1a KD and control BMDM respectively (Fig. 10E). Treatment with 3-MA reduced the proportion of LC3-positive mycobacterial phagosomes in Coro1a KD macrophages (Fig. 10F). These results suggest that autophagosome formation around *M. tuberculosis*-containing phagosomes is also induced in AM and BMDM as a consequence of Coro1a depletion.

Discussion

Coro1a was initially reported being retained on phagosomes containing live mycobacteria, while being rapidly released from phagosomes containing inactive mycobacteria (Ferrari *et al.*, 1999). Genetic depletion or RNA interference-mediated gene silencing of Coro1a was later reported inhibiting the survival of mycobacteria within macrophages (Jayachandran *et al.*, 2007; 2008; Kumar *et al.*, 2010). In this study, we confirmed that the survival

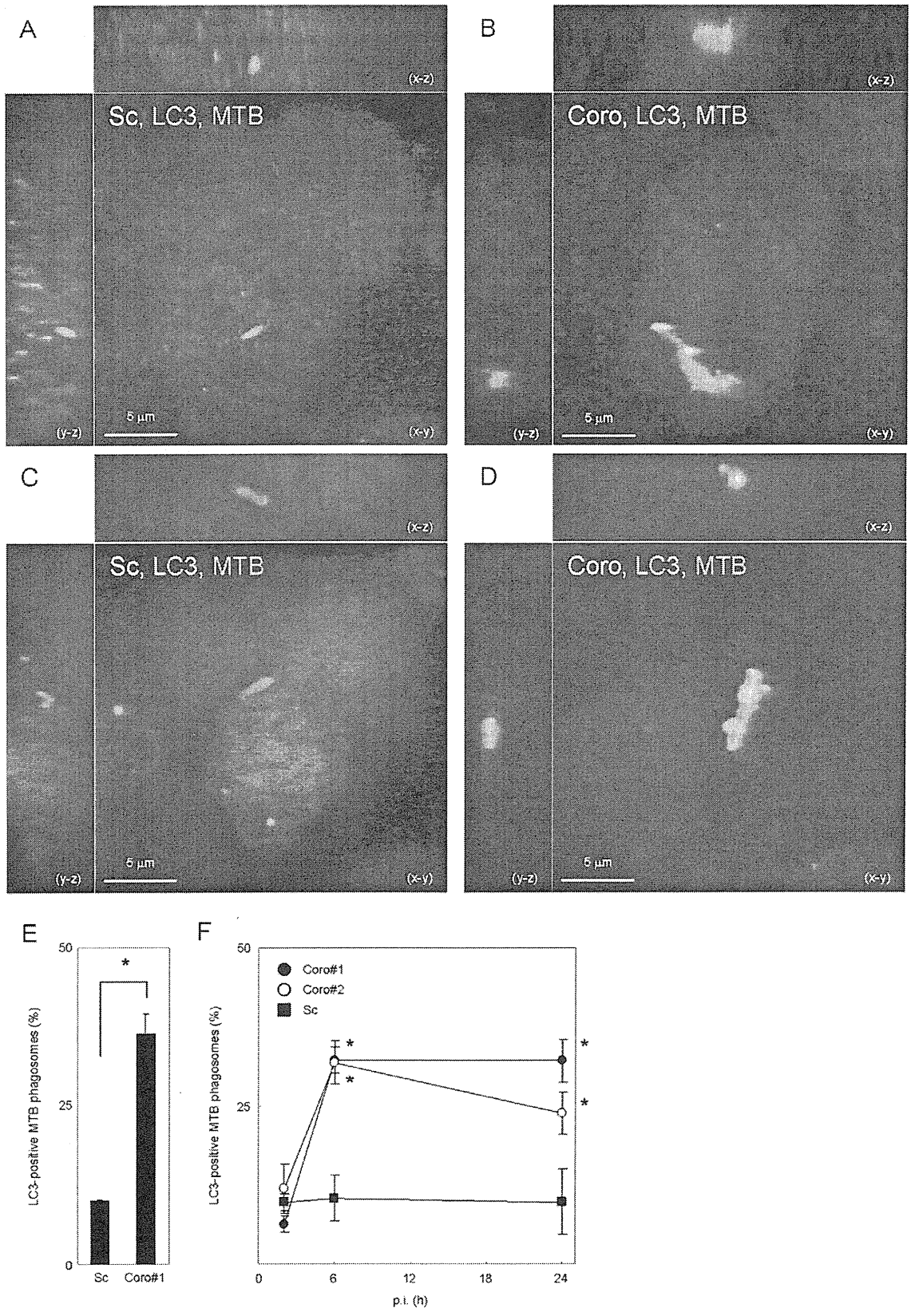
A
Sc, LC3, MTB
(x-z)
(y-z)
5 μm
(x-y)
B
Coro, LC3, MTB
C
Sc, LC3, MTB
D
Coro, LC3, MTB
E
LC3-positive MTB phagosomes (%)
50
25
0
Sc
Coro#1
F
Coro#1
Coro#2
Sc
0
6
12
18
24
p.i. (h)

Fig. 4. LC3 recruitment to mycobacterial phagosomes in Coro1a KD macrophages.
A and B. LC3 recruitment to *M. tuberculosis*-containing phagosomes in Coro1a KD macrophages by immunofluorescence microscopy. Macrophages transfected with scrambled (A) or Coro1a-specific (B) siRNA were infected with DsRed-expressing *M. tuberculosis* for 6 h. Infected macrophages were fixed and stained with anti-LC3 antibody, and then observed with LSCM. Projections of focal planes with y–z and x–z side views are represented.
C and D. Recruitment of LC3 fused with EGFP (EGFP-LC3) to *M. tuberculosis*-containing phagosomes in Coro1a KD macrophages. Macrophages stably expressing EGFP-LC3 were transfected with scrambled (C) or Coro1a-specific (D) siRNA and infected with DsRed-expressing *M. tuberculosis* for 6 h. Infected macrophages were fixed and observed by LSCM. Projections of focal planes with y–z and x–z side views are represented.
E. The proportion of *M. tuberculosis*-containing phagosomes labelled with anti-LC3 antibody in Coro1a KD macrophages. Macrophages transfected with Coro1a-specific or scrambled siRNA were infected with DsRed-expressing *M. tuberculosis* for 6 h. Cells were then stained with anti-LC3 antibody and observed with LSCM. The number of LC3-positive *M. tuberculosis*-containing phagosomes was counted.
F. The proportion of *M. tuberculosis*-containing phagosomes labelled with EGFP-LC3. Macrophages stably expressing EGFP-LC3 were transfected with Coro1a or scrambled siRNA and infected with DsRed-expressing *M. tuberculosis* for 2, 6 and 24 h. Cells were fixed and observed with LSCM. The numbers of LC3-positive mycobacterial phagosomes were counted.
Data represent the mean and SD of three independent experiments in which more than 200 phagosomes were counted for each condition. $^*P < 0.05$ (unpaired Student's *t*-test). Sc, scrambled; Coro, Coro1a; MTB, *M. tuberculosis*.

of *M. tuberculosis* was inhibited in Coro1a KD macrophages (Fig. 1). However, the infection rate of *M. tuberculosis* with Coro1a KD macrophages possibly affects its proliferation within infected macrophages, because a previous study demonstrated that the expression of a dominant-negative form of Coro1a or transfection of Coro1a siRNA decreased the activity of phagocytosis (Yan *et al.*, 2005). To address this possibility, we examined the phagocytosis rate of latex beads and the infection rate of *M. tuberculosis* in Coro1a KD macrophages but found no differences in these events between Coro1a KD and control macrophages (Fig. S2). Previous studies demonstrated that the phagolysosome biogenesis of mycobacterial phagosomes occurred by the depletion of Coro1a in macrophages (Jayachandran *et al.*, 2007; 2008). We also found that the acidification and the fusion of lysosomes with mycobacterial phagosomes were promoted in Coro1a KD macrophages (Fig. 2). However, there has been no direct evidence that the inhibition of mycobacterial proliferation in Coro1a KD macrophages is caused by the promotion of phagolysosome biogenesis.

We hypothesized that autophagy is induced in Coro1a KD macrophages and inhibits *M. tuberculosis* survival. This is because the inhibition of autophagy by 3-MA or gene silencing of autophagy-related genes restores the mycobacterial survival in Coro1a KD macrophages (Fig. 3). To verify this hypothesis, we examined the localization of LC3 and found that LC3 was recruited to *M. tuberculosis*-containing phagosomes in Coro1a KD macrophages (Fig. 4). Thin-section electron microscopy revealed that *M. tuberculosis*-containing phagosomes were surrounded by characteristic autophagic membrane structures in Coro1a KD macrophages (Fig. 5). Treatment with 3-MA or silencing of autophagy-related genes inhibited the recruitment of LC3 to *M. tuberculosis*-containing phagosomes in Coro1a KD macrophages (Fig. 6). It is reported that the delivery of anti-bactericidal protein and/or peptides to mycobacterial phagosomes depended on the induction of autophagy (Alonso *et al.*, 2007; Yuk *et al.*, 2009; Ponpuak *et al.*, 2011). We also showed that the proportion of LC3-positive mycobacterial phagosomes colocalized with p62, ubiquitin and LAMP1 increased in Coro1a KD macrophages up to 24 h p.i., suggesting the involvement of the ubiquitin system and autophagic degradation. Combined, these results suggest that the inhibition of mycobacterial proliferation in Coro1a KD macrophages is caused by the autophagosome formation around mycobacterial phagosomes and subsequent bactericidal effector mechanisms.

In the present study, we sought key events for the induction of autophagosome formation around *M. tuberculosis*-containing phagosomes induced by Coro1a depletion. Immunoblot analysis using whole-cell lysates revealed that the *M. tuberculosis* infection itself did not stimulate whole-cell LC3 processing in Coro1a KD macrophages (Fig. 7 and Fig. S1), because there was no difference in autophagic flux between control and Coro1a KD macrophages infected with *M. tuberculosis* (Fig. 7). Immunofluorescence microscopy also demonstrated that *M. tuberculosis* infection did not induce the formation of punctuated LC3 structures in Coro1a KD macrophages (Fig. 4). In addition, *M. tuberculosis* is thought to prevent the induction of autophagy by inhibiting PI3-kinase activation via the bacterial cell wall component, lipoarabinomannan or a secreted phosphatase (Vergne *et al.*, 2003; 2004; Deretic *et al.*, 2004; 2006). Present results suggest that *M. tuberculosis* infection itself cannot induce autophagy within the cytosol of Coro1a KD macrophages unlike nutrient starvation or pharmacological autophagy inducers.

It is reported that Coro1a regulated the activity of calcineurin and that the calcineurin inhibitors stimulated the fusion of lysosomes with mycobacterial phagosomes (Jayachandran *et al.*, 2007). In *Caenorhabditis elegans*, a loss-of-function or null mutation of calcineurin induces the autophagosome formation (Dwivedi *et al.*, 2009). These results imply that autophagosome formation around mycobacterial phagosomes is caused by the inhibition of

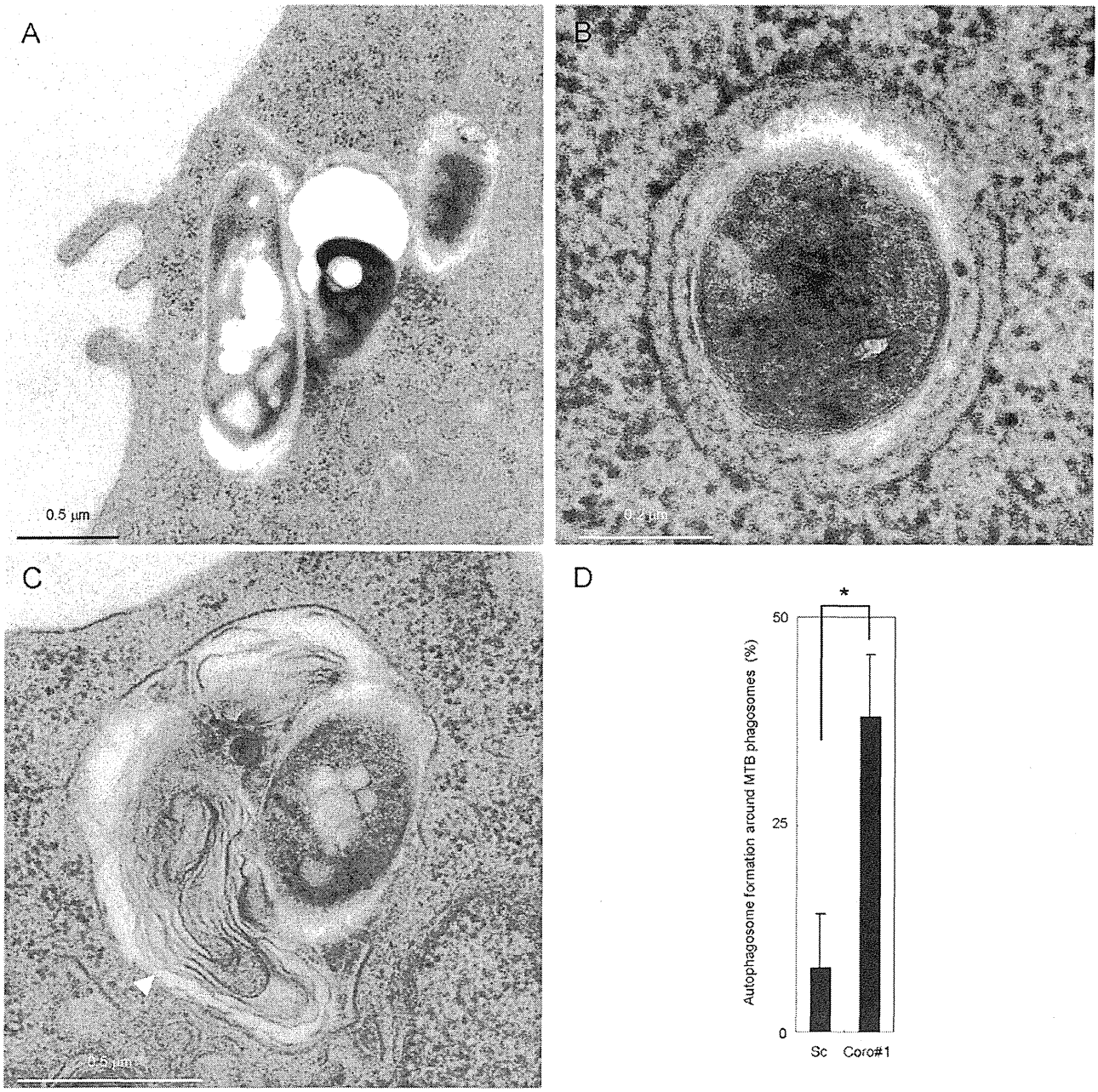

Fig. 5. Thin-section electron micrographs of Coro1a KD macrophages infected with *M. tuberculosis*.
A–C. Macrophages were transfected with scrambled (A) or Coro1a-specific (B, C) siRNA and then infected with *M. tuberculosis* for 6 h. Infected macrophages were fixed and observed with thin-section electron microscopy. An arrowhead indicates the internal membrane in the mycobacterial phagosome.
D. The proportion of *M. tuberculosis*-containing phagosomes associated with multiple membrane structures in Coro1a KD macrophages. Macrophages transfected with Coro1a-specific or scrambled siRNA were infected with *M. tuberculosis* for 6 h. Cells were fixed and observed with thin-section electron microscopy. The number of *M. tuberculosis*-containing phagosomes with multiple membrane structures was counted. Data represent the mean and SD of three independent experiments in which more than 50 phagosomes were counted for each condition.
*$P < 0.05$ (unpaired Student's *t*-test). Sc, scrambled; Coro, Coro1a; MTB, *M. tuberculosis*.

calcineurin activity in Coro1a KD macrophages. We examined whether the inhibition of calcineurin activity induced the autophagosome formation around *M. tuberculosis*-containing phagosomes but found no induction of LC3 recruitment to the phagosomes in macrophages treated with FK506 or cyclosporine A (Fig. S3). Bcl-2 is a member of the anti-apoptotic proteins and interacts with Beclin1 to inhibit the induction of autophagy (Pattingre *et al.*, 2005). The expression of Bcl-2 is reduced in naïve T cells from Coro1a-deficient mice (Mueller *et al.*, 2011). We therefore

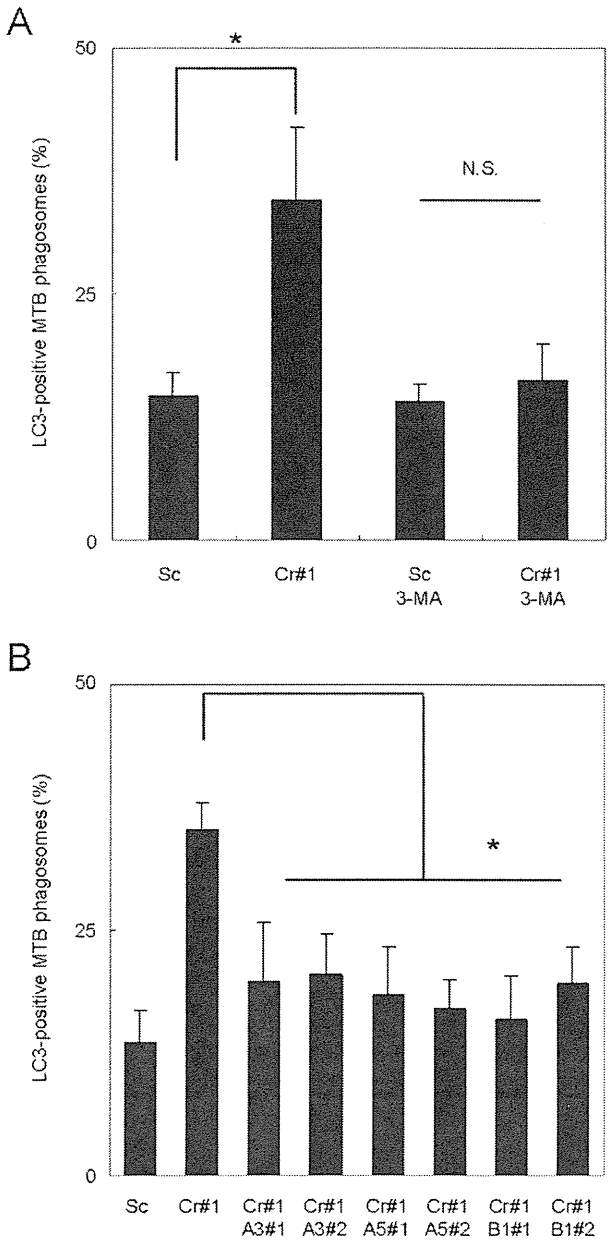

Fig. 6. LC3 recruitment to *M. tuberculosis*-containing phagosomes in Coro1a KD macrophages treated with 3-MA or siRNA for autophagy-related genes. The proportion of LC3-positive mycobacterial phagosomes in Coro1a KD macrophages treated with 3-MA at 10 mM (A) or transfected with siRNA for autophagy-related genes (B). Data represent the mean and SD of three independent experiments in which more than 200 phagosomes were counted for each condition. $^*P < 0.05$; N.S., not significant (unpaired Student's *t*-test). Sc, scrambled; Cr, Coro1a; A3, Atg3; A5, Atg5; B1, Beclin1.

addressed whether autophagosome formation around *M. tuberculosis*-containing phagosomes by Coro1a depletion is accompanied by the downregulation of Bcl-2 and found no significant change in Bcl-2 expression between control and Coro1a KD macrophages (Fig. S4). It is also reported that the transcription of Coro1a is downregulated by the combination of vitamin D3 and retinoic acid in human macrophages (Anand and Kaul, 2003). Vitamin D3 is also reported inducing autophagy in monocyte, resulting in the elimination of infected mycobacteria (Yuk *et al.*, 2009). These reports imply that vitamin D3 decreases the expression of Coro1a in mycobacteria-infected macrophages, leading the autophagosome formation and elimination of infected mycobacteria.

A recent report demonstrated that LC3 is recruited to *Mycobacterium marinum*-containing phagosomes depending on the function of ESX-1 (Lerena and Colombo, 2011). ESAT-6 homologue of *M. marinum* has a pore formation activity in phagosomal membranes and assists the bacilli to escape from phagosomes to cytosol and move by actin-based motility (Stamm *et al.*, 2003; Gao *et al.*, 2004; Smith *et al.*, 2008). *M. tuberculosis* is also reported to translocate from its containing phagosomes to cytosols in infected monocytes depending on ESX-1 secretion system (van der Wel *et al.*, 2007), suggesting that the secreted proteins including ESAT-6 by ESX-1 system damage the phagosomal membranes. Since Coro1a interacts with F-actin to stabilize the structure (Galkin *et al.*, 2008), it is likely that Coro1a localization to mycobacterial phagosomes (Ferrari *et al.*, 1999) supports the phagosomal membranes and that the depletion of Coro1a increases the susceptibility of the phagosomal membranes to ESAT-6 secreted by *M. tuberculosis*. The damage on the membrane of *M. tuberculosis*-containing phagosome could induce the autophagosome formation (Lerena *et al.*, 2010) in Coro1a KD macrophages.

We examined the activation of MAPK signalling pathways involved in autophagosome formation around mycobacterial phagosomes in Coro1a KD macrophages (Fig. 9), as they are involved in autophagy induction (Esclatine *et al.*, 2009). Activation of p38 is indispensable for the induction of autophagy via Toll-like receptor signalling pathways in innate immunity (Xu *et al.*, 2007). JNK signalling pathway was previously reported being involved in the induction of autophagy in macrophages infected with the *eis*-deletion mutant of *M. tuberculosis* (Shin *et al.*, 2010). We assessed the phosphorylation of three MAPKs (ERK-1/2, JNK and p38) and found that only the p38 pathway was specifically activated by *M. tuberculosis* infection in Coro1a KD macrophages (Fig. 9). These results suggest that Coro1a blocks the signal(s) for p38 MAPK activation in response to *M. tuberculosis* infection.

AM are the first defence line of the lung against *M. tuberculosis* infection (Russell, 2001; 2007). We found that the depletion of Coro1a induced autophagosome formation surrounding *M. tuberculosis*-containing phagosomes also in AM and BMDM (Fig. 10). These results suggest that the inhibition of autophagosome formation by

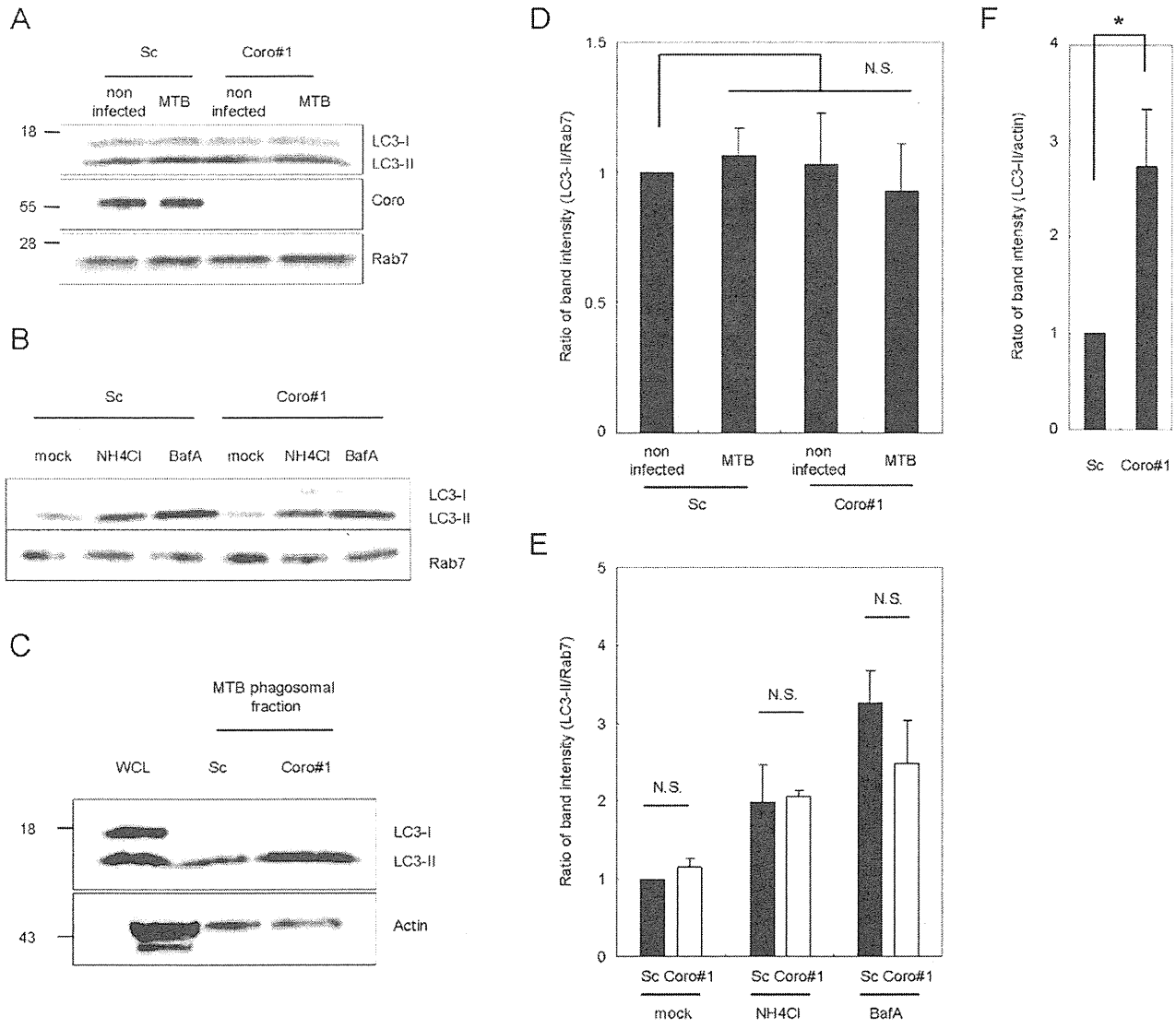

Fig. 7. Immunoblot analysis of LC3 in Coro1a KD macrophages infected with *M. tuberculosis*.
A. Monitoring LC3 processing in Coro1a KD macrophages infected with *M. tuberculosis*. Macrophages transfected with Coro1a-specific or scrambled siRNA were infected with *M. tuberculosis* for 6 h. Whole-cell lysates from non-infected or infected macrophages were subjected to SDS-PAGE, followed by immunoblot analysis using the indicated antibodies.
B. Autophagic flux in Coro1a KD macrophages infected with *M. tuberculosis*. Macrophages transfected with Coro1a-specific or scrambled siRNA were infected with *M. tuberculosis* for 6 h. Infected macrophages were then treated with NH_4Cl (10 mM) or Bafilomycin A1 (10 nM) for 2 h. Whole-cell lysates were subjected to SDS-PAGE, followed by immunoblot analysis using the indicated antibodies.
C. LC3 recruitment to isolated mycobacterial phagosomes. Macrophages transfected with Coro1a or scrambled siRNA were infected with *M. tuberculosis* for 6 h, and phagosomal fractions were isolated as previously described (Beatty *et al.*, 2002; Seto *et al.*, 2011). Whole-cell lysates and phagosomal fractions were subjected to SDS-PAGE, followed by immunoblot analysis using the indicated antibodies.
D–F. Quantification of band intensity for LC3-II. The quantification of band intensity for LC3-II in (A), (B) and (C) was shown in (D), (E) and (F) respectively. The ratio of the band intensity for LC3-II/Rab7 or actin at each condition to that in the macrophage transfected with scrambled siRNA is shown. The data represent the mean and SD of three independent experiments.
*$P < 0.05$; N.S., not significant (paired Student's *t*-test). MTB, *M. tuberculosis*; Sc, scrambled; Coro, Coro1a; NH4Cl, ammonium chloride (NH_4Cl); BafA, Bafilomycin A1.

Coro1a occurs in various types of macrophages. In conclusion, this study demonstrates that Coro1a regulates the autophagosome formation around *M. tuberculosis*-containing phagosomes and assists the survival of infected mycobacteria in macrophages.

Experimental procedures

Cell and bacterial cultures

Raw264.7 and MH-S macrophage cell lines were obtained from the American Type Culture Collection and maintained at 37°C

under a humidified condition with 5% CO_2 in Dulbecco's modified Eagle's medium (DMEM; Sigma-Aldrich, St. Louis, MO) supplemented with 10% fetal bovine serum (FBS; Invitrogen, Carlsbad, CA), 25 μg ml^{-1} penicillin G and 25 μg ml^{-1} streptomycin. BMDM were differentiated from BALB/c mice bone marrow for 7 days in DMEM supplemented with 20% L929-conditioned medium, 10% FBS and antibiotics. *M. tuberculosis* Erdman was obtained from the Japan Research Institute of Tuberculosis, Tokyo, Japan, and grown to mid-logarithmic phase in 7H9 medium supplemented with 10% Middlebrook ADC (BD Biosciences, San Jose, CA), 0.5% glycerol and 0.05% Tween 80 (*Mycobacterium* complete medium) at 37°C. Mycobacteria transformed with a plasmid encoding DsRed were grown in *Mycobacterium* complete medium containing 25 μg ml^{-1} kanamycin.

RNA interference

siRNA duplexes were synthesized by Sigma-Aldrich according to the following sequences: Coro1a#1, sense 5′-GACUGGA CGAGUAGACAAGTT-3′, antisense 5′-CUUGUCUACUCGUCC AGUCTT-3′ (Jayachandran *et al.*, 2008); Coro1a#2 sense 5′-GCAAGACUGGACGAGUAGATT-3′, antisense 5′-UCUACU CGUCCAGUCUUGCTT-3′; Atg3#1, sense 5′-GGUGUAAACA GAUGGAGUATT-3′, antisense 5′-UACUCCAUCUGUUUACACC TT-3′; Atg3#2, sense 5′-GCAUAUCUUCCGACAGACATT-3′, antisense 5′-UGUCUGUCGGAAGAUAUGCTT-3′; Atg5#1, sense 5′-GCUUUACUCUCUAUCAGGATT-3′, antisense 5′-UC CUGAUAGAGAGUAAAGCTT-3′; Atg5#2, sense 5′-GAGACAA GAAGAUGUUAGUTT-3′, antisense 5′-ACUAACAUCUUCUUG UCUCTT-3′; Beclin1#1, sense 5′-GAAAGAUGCUUUAA AUUAATT-3′, antisense 5′-UUAAUUUAAAGCAUCUUUCTT-3′. Beclin1#2, sense 5′-CUGAGAAUGAAUGUCAGAATT-3′, antisense 5′-UUCUGACAUUCAUUCUCAGTT-3′; Mission siRNA universal negative control (Sigma-Aldrich) was used as scrambled siRNA. Transfection of macrophages with siRNA duplexes was performed using Lipofectamine RNAiMAX (Invitrogen) according to the manufacturer's instructions.

Colony-forming unit (cfu) assay

Macrophages transfected with siRNA were grown in 24-well plates at 1×10^5 cells for 24 h, and subsequently infected with *M. tuberculosis* at an moi of 10 for 4 h. Infected macrophages were washed with DMEM three times to remove non-infected mycobacteria and then incubated with DMEM and 10% FBS. At 4 and 72 h p.i., infected macrophages were lysed with 1% IGEPAL in phosphate-buffed saline (PBS), serially diluted with *Mycobacterium* complete medium, and inoculated onto 7H10 agar medium supplemented with 10% Middlebrook OADC (BD Biosciences) and 0.5% glycerol. Colony-forming unit was determined as the mean of four plates at each time point.

Antibodies

Rabbit anti-Coro1a polyclonal antibody (Sigma-Aldrich), mouse anti-actin monoclonal antibody (Sigma-Aldrich), rat anti-mouse LAMP1 monoclonal antibody (SouthernBiotech, Birmingham, AL), mouse anti-LC3 monoclonal antibody (MBL, Nagoya, Japan), rabbit anti-LC3 polyclonal antibody (Sigma-Aldrich), rabbit anti-Atg3 polyclonal antibody (Sigma-Aldrich), rabbit anti-Atg5 polyclonal antibody (Sigma-Aldrich), rabbit anti-Beclin1 polyclonal antibody (Sigma-Aldrich), rabbit anti-p62 polyclonal antibody (MBL), mouse anti-ubiquitin monoclonal antibody (FK2, MBL), mouse anti-Rab7 monoclonal antibody (Abcam, Cambridge, UK), rabbit anti-phospho-ERK1/2 antibody (CST, Denver, MA), rabbit anti-phospho-p38 antibody (CST), rabbit anti-phospho-JNK antibody (CST) and mouse anti-Bcl-2 monoclonal antibody (BD Biosciences) were used for experiments. Alexa488- and Alexa546-conjugated anti-IgG antibodies (Invitrogen) and horseradish peroxidase-conjugated anti-IgG antibodies (Dako, Glostrup, Denmark) were also commercially purchased.

Immunoblot analysis and fluorescence microscopy

Transfected macrophages were extracted by the cell lysis buffer containing 25 mM Tris-HCl pH 7.6, 150 mM NaCl, 1% NP-40, 1% sodium deoxycholate, 0.1% SDS, 100 μM vanadate and protease inhibitor cocktail (Roche, Mannheim, Germany). For immunoblot analysis, cell lysates were separated by SDS-polyacrylamide gel electrophoresis (SDS-PAGE) and then subjected to immunoblot analysis using anti-Coro1a antibody (1:500 v/v), anti-actin antibody (1:1000 v/v), rabbit anti-LC3 polyclonal antibody (1:250 v/v), anti-Atg3 antibody (1:200 v/v), anti-Atg5 antibody (1:300 v/v), anti-Beclin1 antibody (1:100 v/v), anti-Rab7 antibody (1:300 v/v), phospho-ERK1/2 antibody (1:100 v/v), phospho-p38 antibody (1:100 v/v), phospho-JNK antibody (1:100 v/v) or anti-Bcl-2 antibody (1:100 v/v). Band intensity from three independent experiments was quantified using ImageJ (http://rsbweb.nih.gov/ij/). To label lysosomal vesicles with fluorescent dextran, macrophages were incubated with Alexa488-dextran (Invitrogen) at 100 μg ml^{-1} for 12 h. Labelled cells were washed and chased in fluorescent dextran free DMEM with 10% FBS for 6 h.

Immunofluorescence microscopic analysis was performed as previously described (Seto *et al.*, 2009). Macrophages were stained with anti-LAMP1 antibody (1:10 v/v), mouse anti-LC3 monoclonal antibody (1:10 v/v), anti-p62 antibody (1:10 v/v) or anti-ubiquitin antibody (1:10 v/v). Fluorescence microscopy was performed using a LS-1 laser scanning confocal microscope (LSCM; Yokogawa, Tokyo, Japan).

Transfection of macrophages with plasmid

pEGFP-LC3 plasmid was generously provided by Dr Tamotsu Yoshimori (Osaka University, Suita, Japan) and used to transfect Raw264.7 macrophages using an MP-100 electroporator (Digital Bio Technology, Seoul, Korea), according to the manufacturer's instructions. Transfected macrophages were incubated in DMEM with 10% FBS for 24 h prior to the experiments.

Infection of mycobacteria

Transfected macrophages with siRNA grown for 48 h were scraped and grown on round coverslips in 12-well plates for further 12 h. Mycobacteria were washed three times with PBS containing 0.05% Tween 80 and then suspended in DMEM with 10% FBS at a multiplicity of infection (moi) of 30. Aliquots of

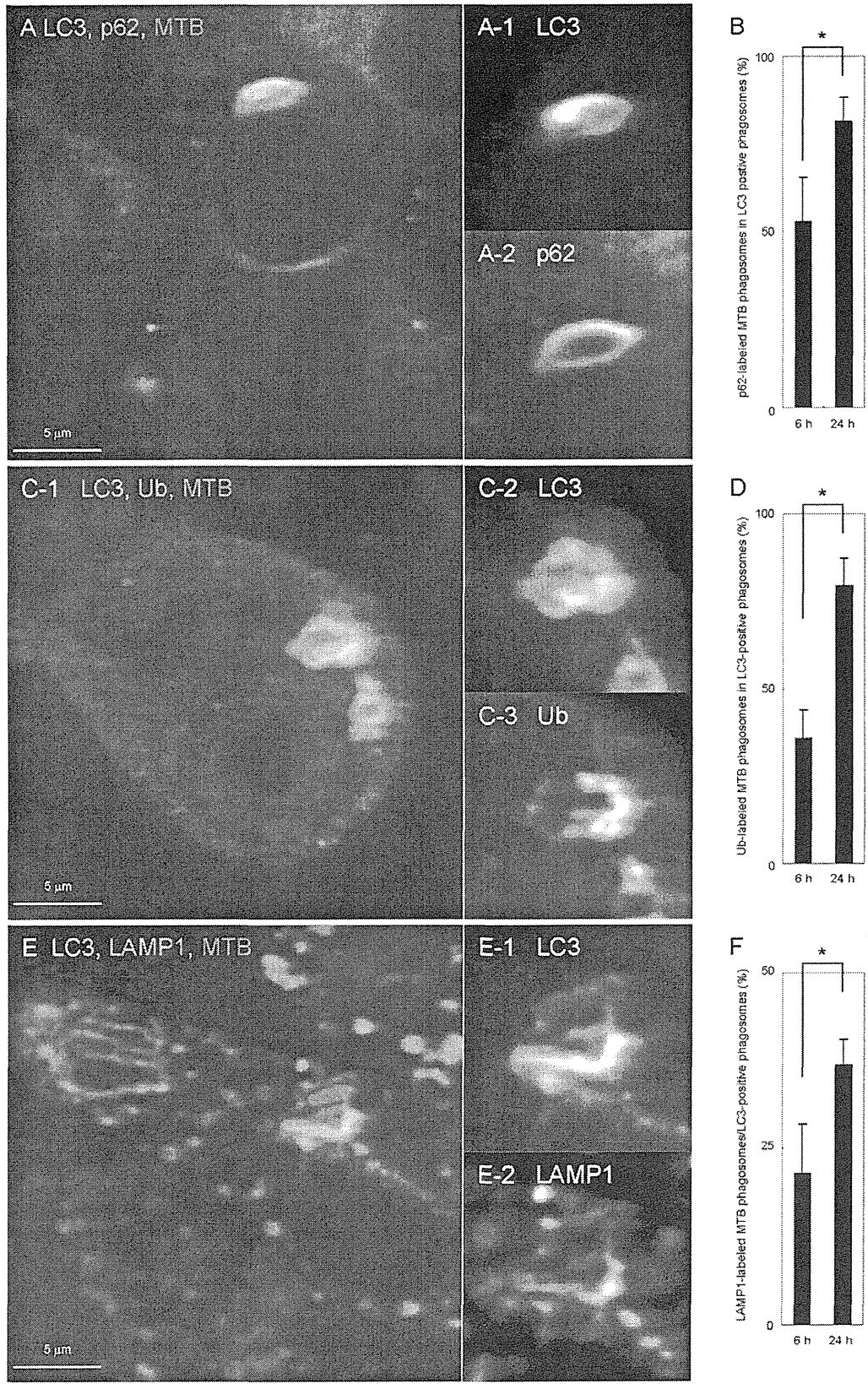
A LC3, p62, MTB
A-1 LC3
A-2 p62
5 μm
B
*
100
50
0
p62-labeled MTB phagosomes in LC3 postive phagosomes (%)
6 h
24 h
C-1 LC3, Ub, MTB
C-2 LC3
C-3 Ub
5 μm
D
*
100
50
0
Ub-labeled MTB phagosomes in LC3-positive phagosomes (%)
6 h
24 h
E LC3, LAMP1, MTB
E-1 LC3
E-2 LAMP1
5 μm
F
*
50
25
0
LAMP1-labeled MTB phagosomes/LC3-positive phagosomes (%)
6 h
24 h

Fig. 8. Recruitment of p62, ubiquitin or LAMP1 to LC3-positive *M. tuberculosis*-containing phagosomes in Coro1a KD macrophages.
A, C and E. Raw264.7 macrophages stably expressing EGFP-LC3 were transfected with Coro1a-specific siRNA for 48 h. Transfected macrophages were infected with Alexa405-labelled *M. tuberculosis* for 24 h and then stained with anti-p62 (A), anti-ubiquitin (C) or anti-LAMP1 (E) antibodies. Enlarged images of A-1, C-1 and E-1 are represented in A-2 and A-3, B-2 and B-3, and C-2 and C-3 respectively.
B, D and F. The proportion of mycobacterial phagosomes labelled with p62 (B), ubiquitin (C) or LAMP1 (F) to the total LC3-positive ones in Coro1a KD macrophages. Macrophages stably expressing EGFP-LC3 were transfected with Coro1a siRNA, and infected with Alexa405-labelled *M. tuberculosis* for 6 or 24 h. Infected macrophages were stained with anti-p62 (B), anti-ubiquitin (D) or anti-LAMP1 (F) antibodies. The numbers of LC3-positive mycobacterial phagosomes labelled with these markers were counted. Data represent the mean and SD of three independent experiments in which more than 100 phagosomes were counted for each condition. $*P < 0.05$ (unpaired Student's *t*-test). Sc, scrambled; Coro, Coro1a; MTB, *M. tuberculosis*; Ub, ubiquitin.

bacterial suspension were added to 3×10^5 cells of Raw264.7 macrophages on coverslips in 12-well plates, followed by centrifugation at 150 *g* for 5 min and incubation for 10 min at 37°C. Infected cells on coverslips were washed three times with DMEM to remove non-phagocytosed bacteria and then incubated with DMEM containing 10% FBS. At the indicated time points, infected cells were fixed with 3% paraformaldehyde in PBS. For immunoblot analysis to detect the phosphorylation of MAPK, macrophages transfected with siRNA grown for 48 h in six-well plates were infected with *M. tuberculosis* at an moi of 30, and then centrifuged for 5 min and incubated for 10 min at 37°C. Infected cells were washed with DMEM to remove non-infected bacteria and then incubated with DMEM containing 10% of FBS. At the indicated time points, infected cells were washed three times with PBS and extracted with the cell lysis buffer.

Thin-section electron microscopy

Raw264.7 macrophages transfected with siRNA in six-well plates were infected with *M. tuberculosis* at an moi of 30 for 2 h, washed three times with DMEM to remove non-infected bacteria, and further incubated in DMEM with 10% FBS for 4 h. Infected macrophages were fixed with 1% glutaraldehyde in 0.1 M cacodylic acid buffer. Fixed macrophages were incubated with 0.1% (w/v) osmium tetroxide. Cells were dehydrated with a series of ethanol washes and treated with propylene oxide. Samples were embedded in Qetol812 resin (OKEN, Tokyo, Japan) according to the manufacturer's protocol. Thin sections were cut with diamond knives and mounted on copper grids. Samples on grids were counter stained with 2% (w/v) uranyl acetate, and then observed with a JEM-1220 electron microscope (JEOL, Tokyo, Japan).

Isolation of M. tuberculosis*-containing phagosomes*

Six 15 cm dishes of Raw264.7 macrophages were used for each condition. Transfection of macrophages with Coro1a or scrambled siRNA was performed using an MP-100 electroporator according to the manufacturer's instructions. Briefly, 6×10^6 Raw264.7 macrophages were transfected with 1.2 nmol of siRNA per plate. Transfected macrophages were incubated in DMEM with 10% FBS for 48 h prior to the experiments. Raw264.7 macrophages transfected with siRNA were infected with mycobacteria at an moi of 30 for 2 h, washed with DMEM three times to remove non-infected mycobacteria, and further incubated in DMEM with 10% FBS for 4 h. Preparation of isolated mycobacterial phagosomes was performed as described previously (Beatty *et al.*, 2002; Seto *et al.*, 2011).

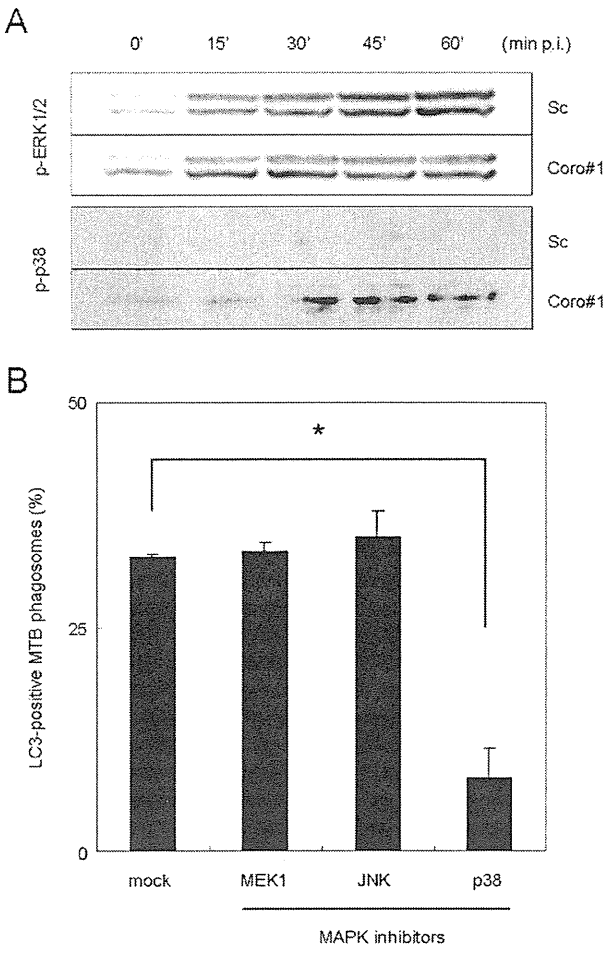

Fig. 9. Differential contribution of MAPK to autophagosome formation around *M. tuberculosis*-containing phagosomes in Coro1a KD macrophages.
A. Phosphorylation of p38 MAPK in Coro1a KD macrophages infected with *M. tuberculosis*. Macrophages transfected with Coro1a-specific or scrambled siRNA were infected with *M. tuberculosis* for the indicated time periods. Whole-cell lysates were subjected to SDS-PAGE, followed by immunoblot analysis using the indicated antibodies.
B. The proportion of LC3-positive *M. tuberculosis*-containing phagosomes in Coro1a KD macrophages treated with MAPK inhibitors. Coro1a KD macrophages expressing EGFP-LC3 were infected with *M. tuberculosis* in the presence of MAPK inhibitors (20 μM) for 6 h. PD98059, SP600125 and SB203580 were used as inhibitors for MEK1, JNK and p38 respectively. Data represent the mean and SD of three independent experiments in which more than 200 phagosomes were counted for each condition. $*P < 0.05$ (unpaired Student's *t*-test). Sc, scrambled; Coro, Coro1a; Mock, solvent control for MAPK inhibitors (0.1% DMSO).

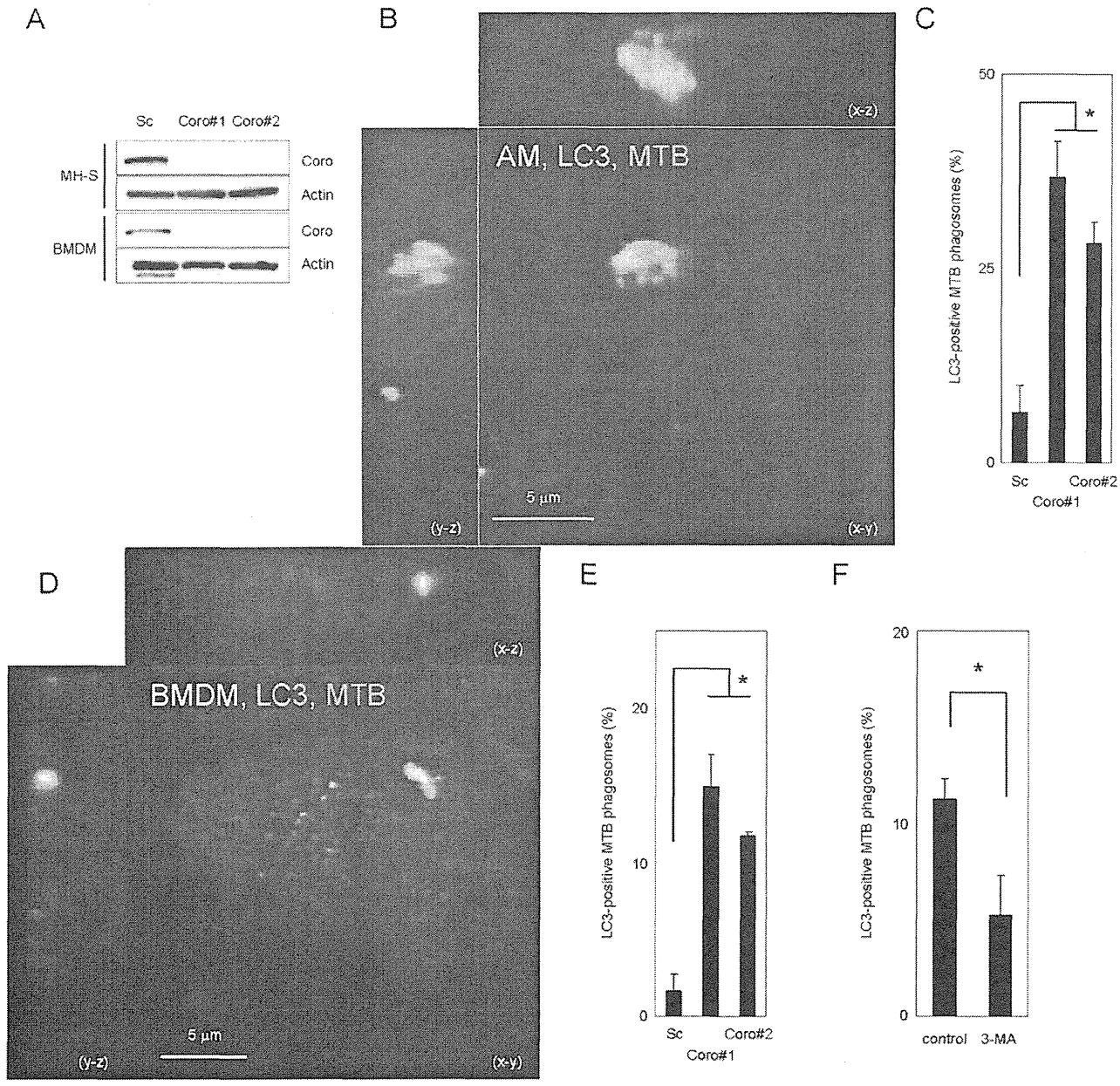

Fig. 10. LC3 recruitment to *M. tuberculosis*-containing phagosomes in the MH-S alveolar macrophage cell line and bone marrow-derived macrophage induced by Coro1a depletion.

A. Immunoblot analysis of MH-S alveolar macrophages (AM) or bone marrow-derived macrophage (BMDM) transfected with Coro1a siRNA. Whole-cell lysates of macrophages transfected with Coro1a or scrambled siRNA were subjected to SDS-PAGE, followed by immunoblot analysis using the indicated antibodies.

B and D. Analysis of LC3 recruitment to *M. tuberculosis*-containing phagosomes in Coro1a KD AM or BMDM. AM (B) or BMDM (D) transfected with Coro1a siRNA were infected with DsRed-expressing *M. tuberculosis* for 6 h. Infected macrophages were fixed and stained with anti-LC3 antibody. Infected macrophages were then observed using LSCM. Projections of focal planes with y–z and x–z side views are represented.

C and E. The proportion of mycobacterial phagosomes labelled with anti-LC3 antibody in AM or BMDM. AM (C) or BMDM (E) were transfected with Coro1a or scrambled siRNA. Transfected macrophages were infected with DsRed-expressing *M. tuberculosis* for 6 h, and then stained with anti-LC3 antibody. LC3-positive phagosomes were counted.

F. 3-MA inhibits the recruitment of LC3 to mycobacterial phagosomes in Coro1a KD BMDM. BMDM were transfected with Coro1a KD siRNA and then treated with or without 3-MA at 10 mM. Macrophages were infected with DsRed-expressing *M. tuberculosis* for 6 h, and then stained with anti-LC3 antibody. The LC3-positive mycobacterial phagosomes were counted. Data represent the mean and SD of three independent experiments in which more than 200 phagosomes were counted for each condition. $^*P < 0.05$ (unpaired Student's *t*-test). Sc, scrambled; Coro, Coro1a; MTB, *M. tuberculosis*; AM, alveolar macrophage cell line MH-S; BMDM, bone marrow-derived macrophage.

Statistics

Paired or unpaired two-sided Student's *t*-tests was used to assess the statistical significance of differences between the two groups. Three or four independent experiments were conducted to assess mycobacterial growth in macrophages, and the number of viable bacteria was determined from the means of four plates. Three independent experiments were conducted to assess the proportions of fluorescence-positive phagosomes.

Acknowledgements

We thank Drs Toshi Nagata and Masato Uchijima (Hamamatsu University School of Medicine, Hamamatsu, Japan) for their helpful discussions. We also thank Ms Keiko Sugaya and Ms Yumiko Suzuki (Hamamatsu University School of Medicine) for their excellent assistance. This work was supported in part by Grants-in-Aid for Young Scientists (B), Scientific Research (B) and Scientific Research (C) from the Japan Society for the Promotion of Science; Scientific Research on Priority Areas from the Ministry of Education, Culture, Sports, Science and Technology of Japan; the Health and Labour Science Research Grants for Research into Emerging and Reemerging Infectious Diseases from the Ministry of Health, Labour and Welfare of Japan; and the United States-Japan Cooperative Medical Science Committee.

References

Alonso, S., Pethe, K., Russell, D.G., and Purdy, G.E. (2007) Lysosomal killing of Mycobacterium mediated by ubiquitin-derived peptides is enhanced by autophagy. *Proc Natl Acad Sci USA* **104:** 6031–6036.

Anand, P.K., and Kaul, D. (2003) Vitamin D3-dependent pathway regulates TACO gene transcription. *Biochem Biophys Res Commun* **310:** 876–877.

Armstrong, J.A., and Hart, P.D. (1971) Response of cultured macrophages to *Mycobacterium tuberculosis*, with observations on fusion of lysosomes with phagosomes. *J Exp Med* **134:** 713–740.

Beatty, W.L., Rhoades, E.R., Hsu, D.K., Liu, F.T., and Russell, D.G. (2002) Association of a macrophage galactoside-binding protein with *Mycobacterium*-containing phagosomes. *Cell Microbiol* **4:** 167–176.

Clemens, D.L., and Horwitz, M.A. (1995) Characterization of the *Mycobacterium tuberculosis* phagosome and evidence that phagosomal maturation is inhibited. *J Exp Med* **181:** 257–270.

Deretic, V., and Levine, B. (2009) Autophagy, immunity, and microbial adaptations. *Cell Host Microbe* **5:** 527–549.

Deretic, V., Vergne, I., Chua, J., Master, S., Singh, S.B., Fazio, J.A., and Kyei, G. (2004) Endosomal membrane traffic: convergence point targeted by *Mycobacterium tuberculosis* and HIV. *Cell Microbiol* **6:** 999–1009.

Deretic, V., Singh, S., Master, S., Harris, J., Roberts, E., Kyei, G., *et al.* (2006) *Mycobacterium tuberculosis* inhibition of phagolysosome biogenesis and autophagy as a host defence mechanism. *Cell Microbiol* **8:** 719–727.

Deretic, V., Delgado, M., Vergne, I., Master, S., De Haro, S., Ponpuak, M., and Singh, S. (2009) Autophagy in immunity against mycobacterium tuberculosis: a model system to dissect immunological roles of autophagy. *Curr Top Microbiol Immunol* **335:** 169–188.

Dupont, N., Lacas-Gervais, S., Bertout, J., Paz, I., Freche, B., Van Nhieu, G.T., *et al.* (2009) Shigella phagocytic vacuolar membrane remnants participate in the cellular response to pathogen invasion and are regulated by autophagy. *Cell Host Microbe* **6:** 137–149.

Dwivedi, M., Song, H.O., and Ahnn, J. (2009) Autophagy genes mediate the effect of calcineurin on life span in *C. elegans*. *Autophagy* **5:** 604–607.

Esclatine, A., Chaumorcel, M., and Codogno, P. (2009) Macroautophagy signaling and regulation. In *Autophagy in Infection and Immunity*. Levine, B., Yoshimori, T., and Deretic, V. (eds). Berlin: Springer, pp. 33–70.

Eskelinen, E.L. (2005) Maturation of autophagic vacuoles in mammalian cells. *Autophagy* **1:** 1–10.

Ferrari, G., Langen, H., Naito, M., and Pieters, J. (1999) A coat protein on phagosomes involved in the intracellular survival of mycobacteria. *Cell* **97:** 435–447.

Galkin, V.E., Orlova, A., Brieher, W., Kueh, H.Y., Mitchison, T.J., and Egelman, E.H. (2008) Coronin-1A stabilizes F-actin by bridging adjacent actin protomers and stapling opposite strands of the actin filament. *J Mol Biol* **376:** 607–613.

Gao, L.Y., Guo, S., McLaughlin, B., Morisaki, H., Engel, J.N., and Brown, E.J. (2004) A mycobacterial virulence gene cluster extending RD1 is required for cytolysis, bacterial spreading and ESAT-6 secretion. *Mol Microbiol* **53:** 1677–1693.

Gutierrez, M.G., Master, S.S., Singh, S.B., Taylor, G.A., Colombo, M.I., and Deretic, V. (2004) Autophagy is a defense mechanism inhibiting BCG and *Mycobacterium tuberculosis* survival in infected macrophages. *Cell* **119:** 753–766.

Hingley-Wilson, S.M., Sambandamurthy, V.K., and Jacobs, W.R., Jr (2003) Survival perspectives from the world's most successful pathogen, *Mycobacterium tuberculosis*. *Nat Immunol* **4:** 949–955.

de Hostos, E.L. (1999) The coronin family of actin-associated proteins. *Trends Cell Biol* **9:** 345–350.

Jagannath, C., Lindsey, D.R., Dhandayuthapani, S., Xu, Y., Hunter, R.L., Jr, and Eissa, N.T. (2009) Autophagy enhances the efficacy of BCG vaccine by increasing peptide presentation in mouse dendritic cells. *Nat Med* **15:** 267–276.

Jayachandran, R., Sundaramurthy, V., Combaluzier, B., Mueller, P., Korf, H., Huygen, K., *et al.* (2007) Survival of mycobacteria in macrophages is mediated by coronin 1-dependent activation of calcineurin. *Cell* **130:** 37–50.

Jayachandran, R., Gatfield, J., Massner, J., Albrecht, I., Zanolari, B., and Pieters, J. (2008) RNA interference in J774 macrophages reveals a role for coronin 1 in mycobacterial trafficking but not in actin-dependent processes. *Mol Biol Cell* **19:** 1241–1251.

Jo, E.K. (2010) Innate immunity to mycobacteria: vitamin D and autophagy. *Cell Microbiol* **12:** 1026–1035.

Kabeya, Y., Mizushima, N., Ueno, T., Yamamoto, A., Kirisako, T., Noda, T., *et al.* (2000) LC3, a mammalian homologue of yeast Apg8p, is localized in autophagosome membranes after processing. *EMBO J* **19:** 5720–5728.

Kumar, D., Nath, L., Kamal, M.A., Varshney, A., Jain, A., Singh, S., and Rao, K.V. (2010) Genome-wide analysis of the host intracellular network that regulates survival of *Mycobacterium tuberculosis*. *Cell* **140:** 731–743.

Lerena, M.C., and Colombo, M.I. (2011) *Mycobacterium marinum* induces a marked LC3 recruitment to its containing phagosome that depends on a functional ESX-1 secretion system. *Cell Microbiol* **13:** 814–835.

Lerena, M.C., Vazquez, C.L., and Colombo, M.I. (2010) Bacterial pathogens and the autophagic response. *Cell Microbiol* **12:** 10–18.

Levine, B. (2005) Eating oneself and uninvited guests: autophagy-related pathways in cellular defense. *Cell* **120:** 159–162.

Mbawuike, I.N., and Herscowitz, H.B. (1989) MH-S, a murine alveolar macrophage cell line: morphological, cytochemical, and functional characteristics. *J Leukoc Biol* **46:** 119–127.

Mizushima, N., and Levine, B. (2010) Autophagy in mammalian development and differentiation. *Nat Cell Biol* **12:** 823–830.

Mueller, P., Liu, X., and Pieters, J. (2011) Migration and homeostasis of naive T cells depends on coronin 1-mediated prosurvival signals and not on coronin 1-dependent filamentous actin modulation. *J Immunol* **186:** 4039–4050.

Pattingre, S., Tassa, A., Qu, X., Garuti, R., Liang, X.H., Mizushima, N., *et al.* (2005) Bcl-2 antiapoptotic proteins inhibit Beclin 1-dependent autophagy. *Cell* **122:** 927–939.

Perrin, A.J., Jiang, X., Birmingham, C.L., So, N.S., and Brumell, J.H. (2004) Recognition of bacteria in the cytosol of mammalian cells by the ubiquitin system. *Curr Biol* **14:** 806–811.

Pethe, K., Swenson, D.L., Alonso, S., Anderson, J., Wang, C., and Russell, D.G. (2004) Isolation of *Mycobacterium tuberculosis* mutants defective in the arrest of phagosome maturation. *Proc Natl Acad Sci USA* **101:** 13642–13647.

Pieters, J. (2008) Coronin 1 in innate immunity. *Subcell Biochem* **48:** 116–123.

Ponpuak, M., Davis, A.S., Roberts, E.A., Delgado, M.A., Dinkins, C., Zhao, Z., *et al.* (2011) Delivery of cytosolic components by autophagic adaptor protein p62 endows autophagosomes with unique antimicrobial properties. *Immunity* **32:** 329–341.

Russell, D.G. (2001) *Mycobacterium tuberculosis*: here today, and here tomorrow. *Nat Rev Mol Cell Biol* **2:** 569–577.

Russell, D.G. (2007) Who puts the tubercle in tuberculosis? *Nat Rev Microbiol* **5:** 39–47.

Seglen, P.O., and Gordon, P.B. (1982) 3-Methyladenine: specific inhibitor of autophagic/lysosomal protein degradation in isolated rat hepatocytes. *Proc Natl Acad Sci USA* **79:** 1889–1892.

Seto, S., Matsumoto, S., Ohta, I., Tsujimura, K., and Koide, Y. (2009) Dissection of Rab7 localization on *Mycobacterium tuberculosis* phagosome. *Biochem Biophys Res Commun* **387:** 272–277.

Seto, S., Matsumoto, S., Tsujimura, K., and Koide, Y. (2010) Differential recruitment of CD63 and Rab7-interacting-lysosomal-protein to phagosomes containing *Mycobacterium tuberculosis* in macrophages. *Microbiol Immunol* **54:** 170–174.

Seto, S., Tsujimura, K., and Koide, Y. (2011) Rab GTPases regulating phagosome maturation are differentially recruited to mycobacterial phagosomes. *Traffic* **12:** 407–420.

Shin, D.M., Jeon, B.Y., Lee, H.M., Jin, H.S., Yuk, J.M., Song, C.H., *et al.* (2010) *Mycobacterium tuberculosis* eis regulates autophagy, inflammation, and cell death through redox-dependent signaling. *PLoS Pathog* **6:** e1001230.

Singh, S.B., Davis, A.S., Taylor, G.A., and Deretic, V. (2006) Human IRGM induces autophagy to eliminate intracellular mycobacteria. *Science* **313:** 1438–1441.

Sirakova, T.D., Dubey, V.S., Kim, H.J., Cynamon, M.H., and Kolattukudy, P.E. (2003) The largest open reading frame (pks12) in the *Mycobacterium tuberculosis* genome is involved in pathogenesis and dimycocerosyl phthiocerol synthesis. *Infect Immun* **71:** 3794–3801.

Smith, J., Manoranjan, J., Pan, M., Bohsali, A., Xu, J., Liu, J., *et al.* (2008) Evidence for pore formation in host cell membranes by ESX-1-secreted ESAT-6 and its role in *Mycobacterium marinum* escape from the vacuole. *Infect Immun* **76:** 5478–5487.

Stamm, L.M., Morisaki, J.H., Gao, L.Y., Jeng, R.L., McDonald, K.L., Roth, R., *et al.* (2003) *Mycobacterium marinum* escapes from phagosomes and is propelled by actin-based motility. *J Exp Med* **198:** 1361–1368.

Sugaya, K., Seto, S., Tsujimura, K., and Koide, Y. (2011) Mobility of late endosomal and lysosomal markers on phagosomes analyzed by fluorescence recovery after photobleaching. *Biochem Biophys Res Commun* **410:** 371–375.

Vergne, I., Chua, J., and Deretic, V. (2003) *Mycobacterium tuberculosis* phagosome maturation arrest: selective targeting of PI3P-dependent membrane trafficking. *Traffic* **4:** 600–606.

Vergne, I., Chua, J., Singh, S.B., and Deretic, V. (2004) Cell biology of *Mycobacterium tuberculosis* phagosome. *Annu Rev Cell Dev Biol* **20:** 367–394.

van der Wel, N., Hava, D., Houben, D., Fluitsma, D., van Zon, M., Pierson, J., *et al.* (2007) *M. tuberculosis* and *M. leprae* translocate from the phagolysosome to the cytosol in myeloid cells. *Cell* **129:** 1287–1298.

World Health Organization (2010) *WHO Report 2010 Global Tuberculosis Control*. Geneva: WHO [WWW document]. http://www.who.int/tb/publications/global_report/2010/en/index.html.

Xu, Y., Jagannath, C., Liu, X.D., Sharafkhaneh, A., Kolodziejska, K.E., and Eissa, N.T. (2007) Toll-like receptor 4 is a sensor for autophagy associated with innate immunity. *Immunity* **27:** 135–144.

Yan, M., Collins, R.F., Grinstein, S., and Trimble, W.S. (2005) Coronin-1 function is required for phagosome formation. *Mol Biol Cell* **16:** 3077–3087.

Yuk, J.M., Shin, D.M., Lee, H.M., Yang, C.S., Jin, H.S., Kim, K.K., *et al.* (2009) Vitamin D3 induces autophagy in human monocytes/macrophages via cathelicidin. *Cell Host Microbe* **6:** 231–243.

Zheng, Y.T., Shahnazari, S., Brech, A., Lamark, T., Johansen, T., and Brumell, J.H. (2009) The adaptor protein p62/

SQSTM1 targets invading bacteria to the autophagy pathway. *J Immunol* **183:** 5909–5916.

Supporting information

Additional Supporting Information may be found in the online version of this article:

Fig. S1. Immunoblot analysis of LC3 in macrophages infected with *M. tuberculosis* at deferent moi.
A. Raw264.7 macrophages were transfected with Coro1a-specific or scrambled siRNA. Transfected macrophages were infected with *M. tuberculosis* at different moi for 6 h. Whole-cell lysates were subjected to SDS-PAGE, followed by immunoblot analysis using the indicated antibodies.
B. The band intensity for LC3-II per Rab7 at each condition to that in the macrophage without infection is shown. The data represent the mean and SD of three independent experiments. N.S., not significant (paired Student's *t*-test); MTB, *M. tuberculosis*; Sc, scrambled; Coro, Coro1a.
Fig. S2. Phagocytosis of latex beads and infection by *M. tuberculosis* in Coro1a KD macrophage. Raw264.7 macrophages were transfected with Coro1a-specific or scrambled siRNA for 48 h. Transfected macrophages were phagocytosed by FITC-labelled latex beads or DsRed-expressing *M. tuberculosis*. The rate of phagocytosed or infected macrophages were analysed by flow cytometry or fluorescent microscopy respectively. The data represent the mean and SD of three independent experiments. N.S., not significant (paired Student's *t*-test); MTB, *M. tuberculosis*; Sc, scrambled; Coro, Coro1a.
Fig. S3. LC3 recruitment to mycobacterial phagosomes in macrophages treated with calcineurin inhibitors. Macrophages stably expressing EGFP-LC3 were treated with FK506 (0.5 μM) or cyclosporine A (0.1 μM) for 1 h, and then infected with DsRed-expressing *M. tuberculosis* for 6 h. Cells were fixed and observed with LSCM. The number of LC3-positive *M. tuberculosis* phagosomes was counted. Data represent the mean and SD of three independent experiments in which more than 200 phagosomes were counted for each condition. N.S., not significant (unpaired Student's *t*-test); FK, FK506; Cyc, cyclosporine A; MTB, *M. tuberculosis*.
Fig. S4. Bcl-2 expression in Coro1a KD macrophages. Raw264.7 macrophages were transfected with Coro1a-specific siRNA for 48 h. Whole-cell lysates were subjected to SDS-PAGE, followed by immunoblot analysis using anti-Bcl-2 or anti-Coro1a antibodies. Bec1, Beclin1; Sc, scrambled; Coro, Coro1a.

Please note: Wiley-Blackwell are not responsible for the content or functionality of any supporting materials supplied by the authors. Any queries (other than missing material) should be directed to the corresponding author for the article.

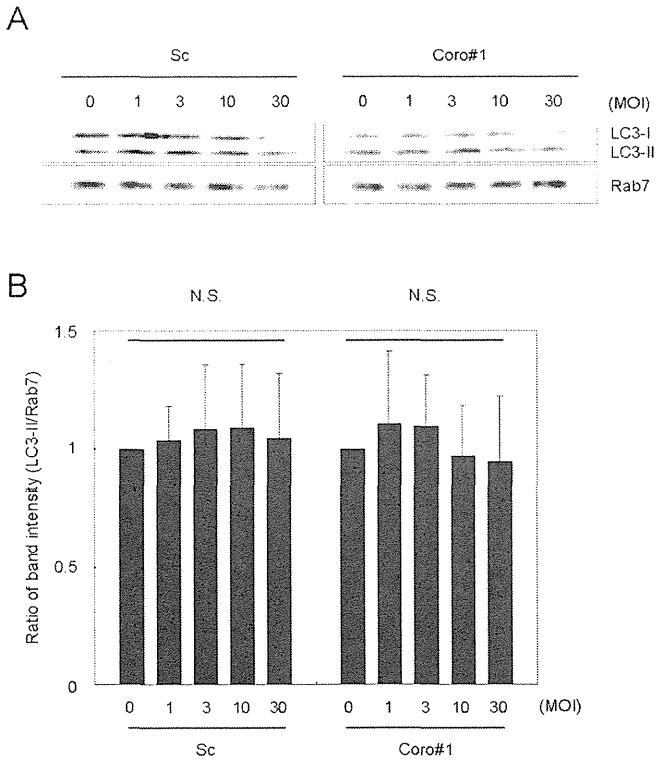

Fig. S1. Seto et al

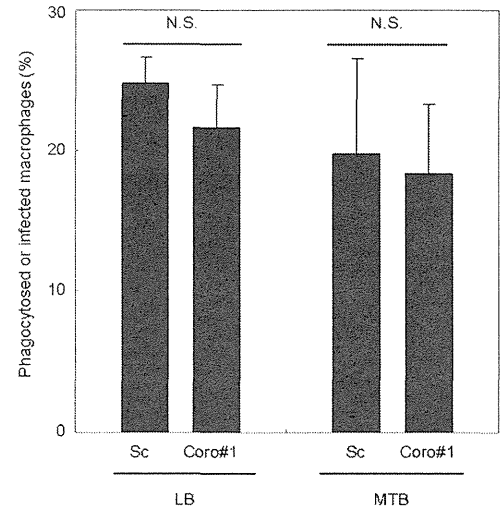

Fig. S2. Seto et al

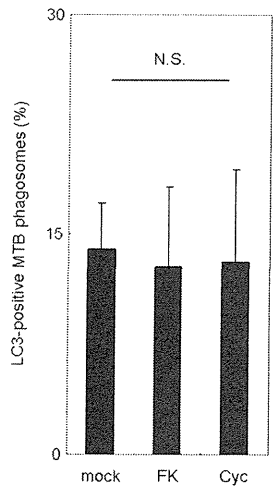

Fig. S3. Seto et al

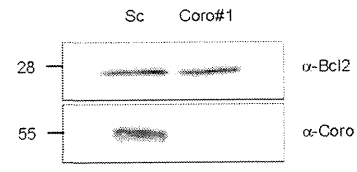

Fig. S4. Seto et al

生体の科学　63(5)：494-495，2012

8．ファゴソーム

アクチン結合性タンパク質 Coronin-1a による結核菌ファゴソームへのオートファゴソーム形成阻害機構

瀬戸真太郎　辻村邦夫　堀井俊伸　小出幸夫

●Coronin ファミリー遺伝子と Coronin-1a の構造

Coronin-1a は Coronin ファミリー遺伝子に属するアクチン結合性タンパク質である[1]。Coronin ファミリー遺伝子は酵母から哺乳類まで多くの真核生物に保存されている。Coronin は粘菌のアクチン/ミオシン複合体に結合するタンパク質として単離されて，粘菌細胞の王冠状突起に局在することから Coronin と命名された。Coronin はアクチンの枝分かれ構造に機能する Arp2/3 複合体と結合することによって，Arp2/3 のアクチン繊維からの離脱を制御している。粘菌や酵母では Coronin は 1 遺伝子しか存在しないが，ヒトやマウスでは 7 遺伝子存在する。

結晶構造解析[2]などによって Coronin-1a の立体構造は明らかになっている。N 末端側は 7 枚のβプロペラによって構成されている。これらのβプロペラは五つの WD リピートと，その後に続く二つのβシート構造から形成されている。C 末端側はコイルドコイル構造によって構成されている。このコイルドコイル構造によって Coronin-1a は三量体を形成している。さらに，C 末端側でアクチン繊維と結合する。

●結核菌ファゴソームにおける Coronin-1a の局在と機能

Coronin-1a はヒトおよびマウスでは主に白血球系細胞で発現している。マクロファージにおける Coronin-1a の機能が明らかになったのは，結核菌ファゴソームに局在するタンパク質として同定された TACO (tryptophan aspartate containing coat protein)[3]によってである。

結核菌は典型的な細胞内寄生性細菌であり，貪食されたマクロファージ内で増殖することができる。この細胞内増殖能は結核菌ファゴソームとリソソームの融合(ファゴリソソーム形成)を阻害することによって獲得している。Pieters らは結核ワクチン株である BCG をマクロファージに感染させて，生化学的に BCG ファゴソームを単離した。BCG ファゴソームに特異的に局在するタンパク質を探索した結果，TACO すなわち Coronin-1a を同定した。免疫蛍光顕微鏡法によって，Coronin-1a は死菌 BCG ファゴソームには一時的にしか局在しないが，生菌 BCG ファゴソームには継続的に局在していることを明らかにした。以上の結果は，Coronin-1a は結核菌ファゴソームに局在することによってファゴリソソーム形成を阻害することを示唆する。

次に，Coronin-1a ノックアウトマウスを作製して，そのノックアウトマウス由来マクロファージに結核菌を感染させた[4]。Coronin-1a ノックアウトマウス由来マクロファージにおいて，感染結核菌にファゴリソソーム形成が行われること，結核菌の増殖が抑制されることを明らかにした。また，カルシニューリンが Coronin-1a によって活性化されることを見出し，FK506 やサイクロスポリンなどのカルシニューリン阻害剤によって，結核菌ファゴソームはリソソームと融合することを明らかにした。しかし，Coronin-1a の結核菌ファゴソームへの継続的な局在機構やカルシニューリンによるファゴリソソーム形成阻害の分子機構について，その詳細は明らかになっていない。

●Coronin-1a は結核菌へのオートファゴソーム形成を阻害する

オートファジーは飢餓などで誘導されるタンパ

Shintaro Seto, Kunio Tujimura, Toshinobu Horii, Yukio Koide：浜松医科大学 感染症学講座

0370-9531/10/¥500/論文/JCOPY

ク質分解機構であり，細胞や生体の恒常性の維持に機能する。近年，オートファジーは細胞内寄生性細菌の排除にも関与していることが明らかになっている。しかし，結核菌感染マクロファージではオートファジーは誘導されない。筆者らは，結核菌感染マクロファージにおいてCoronin-1aがオートファゴソーム形成を阻害して，その結果，結核菌の細胞内増殖を支持していることを見出した(図)[5]。すなわち，Coronin-1aノックダウンマクロファージにおいて，①結核菌の細胞内増殖は抑制されるが，同時にオートファジー関連遺伝子もノックダウンすると結核菌増殖は回復することを明らかにした。さらに，②結核菌ファゴソームにオートファジーマーカーであるLC3が局在して，結核菌オートファゴソームが形成されること，③LC3陽性結核菌ファゴソームにオートファジーアダプタータンパク質であるp62/SQSTM1が局在して，結核菌ファゴソームのポリユビキチン化が促進されることを明らかにした。また，Coronin-1aノックダウンマクロファージでは結核菌感染によってp38MAPキナーゼが特異的に活性化した。以上の結果は，結核菌感染によって活性化されるオートファジーを誘導するシグナル伝達経路がCoronin-1aによって阻害されている可能性を示唆する。

結核菌はマクロファージに貪食されてもファゴリソソーム形成を阻害するだけでなく，オートファジー誘導も回避して細胞内増殖を行う戦略を採用している。これらの戦略にアクチン結合性タンパク質であるCoronin-1aが関与していることは非常に興味深い。Coronin-1aによるオートファゴソーム形成阻害機構を研究することによって，結核菌による細胞内寄生戦略の分子機構が解明されることを期待できる。

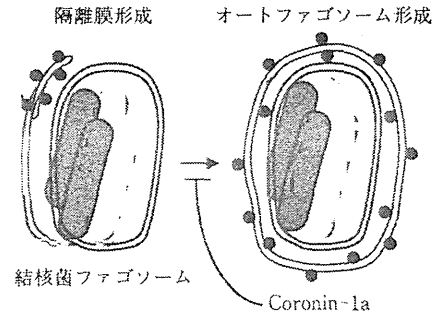

図　Coronin-1aによる結核菌へのオートファゴソーム形成阻害機構
Coronin-1aは隔離膜形成，もしくはオートファゴソーム形成を阻害することによって，結核菌の細胞内増殖を支持している。

文　献

1) de Hostos EL：*Trend Cell Biol* **9**：345-350, 1999
2) Appleton BA et al：*Structure* **14**：87-96, 2006
3) Ferrari G et al：*Cell* **97**：435-447, 1999
4) Jayachandran R et al：*Cell* **130**：37-50, 2007
5) Seto S et al：*Cell Microbiol* **14**：710-727, 2012

INT J TUBERC LUNG DIS 16(5):660–664

http://dx.doi.org/10.5588/ijtld.11.0534
E-published ahead of print 7 March 2012

Long-term radiographic outcome of nodular bronchiectatic *Mycobacterium avium* complex pulmonary disease

S. Kitada, T. Uenami, K. Yoshimura, Y. Tateishi, K. Miki, M. Miki, H. Hashimoto, T. Fujikawa, M. Mori, K. Matsuura, M. Kuroyama, R. Maekura

Department of Respiratory Medicine, National Hospital Organisation National Toneyama Hospital, Osaka, Japan

SUMMARY

BACKGROUND: Although *Mycobacterium avium* complex pulmonary disease (MAC-PD) is a growing health problem, little is known about long-term radiographic outcome and factors for deterioration in patients with MAC-PD.

METHODS: Data on patients with nodular bronchiectatic (NBE) MAC-PD who underwent regular follow-up for >5 years were retrospectively reviewed. Changes in plain chest radiograph (CXR) and baseline characteristics were compared between the stable and deteriorated groups.

RESULTS: Seventy-two patients were investigated, including 30 patients who were examined 10 years after the initial visit. One patient (1.4%) showed progressive or remarkably progressive disease on CXR at 1 year; this rate increased to 22.2% at 5 years and to 53.3% at 10 years. Body mass index (BMI) at the initial visit was lower in the deteriorated group than in the stable group. Cavitary disease and resistance to a macrolide were seen more frequently at the initial visit in the deteriorated group than in the stable group.

CONCLUSIONS: NBE MAC-PD is a slowly but substantially progressive long-term infection (5–10 years). Our data suggest that patients with lower BMI, cavitary disease and resistance to a macrolide at initial visit are more likely to progress to deteriorating disease.

KEY WORDS: non-tuberculous mycobacteria; chest radiography; retrospective cohort study

THE *Mycobacterium avium* complex (MAC), which includes *M. avium* and *M. intracellulare*, causes chronic and progressive lung infection.[1] The incidence of MAC pulmonary disease (MAC-PD) is reportedly increasing in many countries.[2–4] In Japan, the estimated prevalence of non-tuberculous mycobacterial disease was 0.82 per 1 000 000 population in the 1970s and 6.7 in 2005; most of these cases involved MAC-PD.[5,6] Physicians have recently been encountering an increasing number of patients with MAC-PD, and the management of this disease has become a major concern.

Historically, patients with MAC lung disease are typically middle-aged male smokers with apical fibrocavitary disease, as evidenced by chest radiography (CXR).[1] In addition, however, MAC is also known to cause progressive parenchymal lung disease in patients without underlying lung disease.[7] This type of disease is known as nodular-bronchiectatic (NBE) disease (NBE MAC-PD). NBE MAC-PD is characterised radiographically by multifocal bronchiectasis with centrilobular nodules that predominantly involve the right middle lobe and lingula; it is usually observed in thin, elderly females with no history of smoking. Although many physicians report that NBE disease tends to progress much more slowly than fibrocavitary disease, few studies have been published on the long-term outcome of NBE MAC disease. To facilitate its management and identify effective treatment strategies, it is essential to understand the long-term clinical course of the disease. To address this problem, we conducted a retrospective cohort study of patients with NBE MAC-PD in Japan.

STUDY POPULATION AND METHODS

Patient selection

We retrospectively reviewed the medical charts of patients with NBE MAC-PD who first presented after January 1997 and either died or had >5 years of follow-up at the National Hospital Organisation (NHO) National Toneyama Hospital. MAC-PD was diagnosed according to the 1997 guidelines of the American Thoracic Society (ATS).[8] NBE was defined by the presence of multifocal bronchiectasis with multiple nodular shadows on plain chest radiographs (CXRs) and chest computed tomography (CT) images at the time of the initial visit. CT images were obtained from all patients at initial visit or within 1 year of the initial visit. Patients who had underlying structural lung disease were excluded. Structural lung

Correspondence to: Seigo Kitada, Department of Respiratory Medicine, National Hospital Organisation National Toneyama Hospital, Toyonaka-shi, Osaka 560-8522, Japan. Tel: (+81) 6 6853 2001. Fax: (+81) 6 6853 3127. e-mail: kitadase@toneyama.go.jp

Article submitted 5 August 2011. Final version accepted 29 October 2011.

disease was identified in cases in which the patient had previous pulmonary tuberculosis (TB), pneumoconiosis, emphysema, interstitial pneumonia or severe bullae.

The study was approved by the NHO National Toneyama Hospital Institutional Review Board (approval number 1031), which permitted retrospective chart review and anonymous reporting of the results without informed consent from the patients.

Retrospective data collection

Clinical features, including age, sex, body mass index (BMI), underlying conditions, including respiratory and non-respiratory disease, and time since symptom onset were recorded. Identification of MAC species, macrolide resistance, the context and length of treatment for MAC, sputum culture conversion, relapse, mean time to negative culture results and erythrocyte sedimentation rate (ESR) were also recorded. Macrolide susceptibility results were not obtained from patients who first visited the hospital before 2002, as the macrolide susceptibility kit (BrothMIC NTM, Kyokuto Pharmaceutical Industrial, Tokyo, Japan) was not available before 2002 in Japan. Sputum culture was performed using MGIT™ (Mycobacteria Growth Indicator Tube, BD, Sparks, MD, USA) or egg-based Ogawa medium. Sputum conversion was defined as three consecutive negative cultures within 6 months, with the time of conversion defined as the date of the first negative culture. Sputum relapse was defined as two consecutive positive cultures after sputum conversion. The presence of cavitary disease along with NBE on plain CXR and CT was also recorded.

Evaluation of disease progression on chest radiography

The progression of MAC-PD was assessed by comparing the plain CXRs obtained at 1, 5 and 10 years with those from the initial visit. Changes in CXR findings were graded on a five-level scale: improved, unchanged, slightly progressive, progressive and remarkably progressive. Improved disease was defined as shrinkage or disappearance of abnormal shadows on CXR; slightly progressive disease was defined as a slight increase in the size of pre-existing abnormal shadows; progressive disease was defined as an increase in the size of pre-existing abnormal shadows or emergence of new abnormal shadows; and remarkably progressive disease was defined as emergence of consolidation or cavitary lesions in addition to an increase in the size of pre-existing abnormal shadows. All CXR findings were independently interpreted by two expert pulmonologists blinded to other clinical information, and the final interpretation was obtained by consensus.

Patients were categorised into two groups, stable and deteriorated, on the basis of CXR changes. The stable group included patients with evidence of improved, unchanged and slightly progressive disease on CXR, and the deteriorated group included those with progressive and remarkably progressive disease.

Statistical analysis

Variables are expressed as mean ± standard deviation (SD), and categorical values are expressed as number of patients (percentage). Comparisons were performed using the Mann-Whitney *U*-test for continuous variables and the χ^2 test or Fisher's exact test for categorical variables using JMP version 8 statistical software package (SAS Institute, Cary, NC, USA). Significance was defined as $P < 0.05$, and all tests were two-sided.

RESULTS

Patient population

The study population consisted of 72 patients with MAC-PD who died or were followed up for >5 years. Thirty of the patients were observed for 10 years from the initial visit. None were seropositive for the human immunodeficiency virus. Two patients died due to respiratory failure 2.9 (an 80-year-old man) and 6.6 (a 72-year-old woman) years after the initial visit; both had cavitary disease along with nodular bronchiectasis at their initial visit. The baseline characteristics are shown in Table 1. All patients had

Table 1 Baseline characteristics of patients with nodular bronchiectatic *Mycobacterium avium* complex pulmonary disease ($N = 72$)

Characteristic	*n* (%) or mean ± SD
Age, years	62.5 ± 11.4
Female patients	60 (83.3)
Time since symptom onset, years	0.8 ± 2.5
BMI, kg/m^2	19.7 ± 2.9
ESR, mm/h	35.8 ± 22.5
Underlying condition	31 (43.1)
Respiratory disease	1
Non-respiratory disease	30
Cavitary disease	10 (13.9)
MAC species	
M. avium	42 (58.3)
M. intracellulare	15 (20.8)
Both	8 (11.1)
MAC species, non-typable	7 (9.7)
Sputum smear >1+	6 (8.3)
Resistance to a macrolide*	3 (9.7)
Receiving multidrug treatment	44 (61.1)
Mean length of treatment, years	1.9 ± 1.5
Sputum culture conversion with treatment	30 (68.2)
Relapse	23 (76.7)
Mean time during which culture was negative, years	1.5 ± 1.1

*Macrolide resistance (MIC > 32 μg/ml) was checked for 31 patients.
SD = standard deviation; BMI = body mass index; ESR = erythrocyte sedimentation rate; MAC = *Mycobacterium avium* complex; MIC = minimum inhibitory concentration.